Chemistry–A European Journal
Research Article
doi.org/10.1002/chem.202300159
Chemistry Europe
European Chemical Societies Publishing
www.chemeurj.org

Rationalizing the Optimization of Detergents for Membrane Protein Purification

Leonhard H. Urner,*[a, c] Florian Junge,[b] Francesco Fiorentino,[c, d] Tarick J. El-Baba,[c] Denis Shutin,[c] Gideon Nölte,[b] Rainer Haag,[b] and Carol V. Robinson*[c]

Abstract: Membrane protein purification by means of detergents is key to isolating membrane-bound therapeutic targets. The role of the detergent structure in this process, however, is not well understood. Detergents are optimized empirically, leading to failed preparations, and thereby raising costs. Here we evaluate the utility of the hydrophilic-lipophilic balance (HLB) concept, which was introduced by Griffin in 1949, for guiding the optimization of the hydrophobic tail in first-generation, dendritic oligoglycerol detergents ([G1] OGDs). Our findings deliver qualitative HLB guidelines for rationalizing the optimization of detergents. Moreover, [G1] OGDs exhibit strongly delipidating properties, regardless of the structure of the hydrophobic tail, which delivers a methodological enabling step for investigating binding strengths of endogenous lipids and their role for membrane protein oligomerization. Our findings will facilitate the analysis of challenging drug targets in the future.

Introduction

Membrane proteins are molecular machines that account as targets for 50% of current drugs.[1] Lipid membranes surrounding proteins can modulate their structure, function, and drug binding.[2] To recapitulate these effects in membrane models, tools are needed that enable capturing the dynamic lipid environment surrounding proteins.[3] Detergents traditionally enable the purification of protein-lipid complexes from membranes.[4] However, the analysis of individual complexes in solution is a challenge. Condensed-phase techniques, for example, those based on spectroscopy,[5] light-scattering,[6] or crystallography,[7] deliver average results from a population of species within a sample.[8] Upon purification with detergents in solution, proteins and their lipid complexes are in equilibrium, rendering the unambiguous investigation of individual species difficult.[3b,9] Native mass spectrometry (nMS) can help to overcome this challenge. In nMS, proteins and their lipid complexes are transferred out of their solution equilibrium into the vacuum of a mass spectrometer.[10] The detergent environment surrounding proteins is removed by thermal activation.[10] If conditions are identified that allow retaining proteins and their lipid complexes in a stable state, then proteins and their lipid complexes can be detected according to their mass-to-charge ratios. Since lipid binding events can be distinguishable in mass, proteins and their lipid complexes can be investigated separately by nMS. The ability to measure the mass of distinct protein complexes inside a mass spectrometer provides the unique opportunity to investigate the role of lipids for the structure of proteins.[4,8,11]

Detergents that are used for applications at the interface between solution and vacuum ideally keep protein complexes stable in solution and gas phase and are compatible to condensed-phase methods (Figure 1a).[3b,8] In solution, detergents form water-soluble proteomicelles by shielding hydrophobic protein surfaces from water.[12] In the gas phase, the removal of detergents from proteomicelles helps to maintain non-covalent interactions in protein assemblies.[13] Furthermore, the purification of protein-lipid complexes in solution is fine-tuned to avoid an over-saturation of mass spectra with lipids, while preserving sufficient lipid interactions for maintaining protein stability.[4,14] Ideal experimental requirements depend on the nature of each protein complex, often resulting in time-consuming detergent screenings and empirical sample optimization.[10] Approaches to optimize the purification of protein-lipid complexes include varying the concentration of detergents during purification steps,[14b] varying the detergent,[15] and applying purification steps repetitively.[14a,b,16]

[a] Dr. L. H. Urner
TU Dortmund University
Department of Chemistry and Chemical Biology
Otto-Hahn-Str. 6, 44227 Dortmund (Germany)
E-mail: leonhard.urner@tu-dortmund.de
[b] F. Junge, G. Nölte, Prof. Dr. R. Haag
Freie Universität Berlin
Institute of Chemistry and Biochemistry
Takustraße 3, 14195 Berlin (Germany)
[c] Dr. L. H. Urner, Dr. F. Fiorentino, Dr. T. J. El-Baba, Dr. D. Shutin, Prof. Dr. C. V. Robinson
Kavli Institute for Nanoscience Discovery
South Parks Rd, OX1 3QU Oxford (UK)
E-mail: carol.robinson@chem.ox.ac.uk
[d] Dr. F. Fiorentino
Department of Drug Chemistry and Technologies
Sapienza University of Rome
P.le A. Moro 5, 00185 Rome (Italy)

Supporting information for this article is available on the WWW under https://doi.org/10.1002/chem.202300159

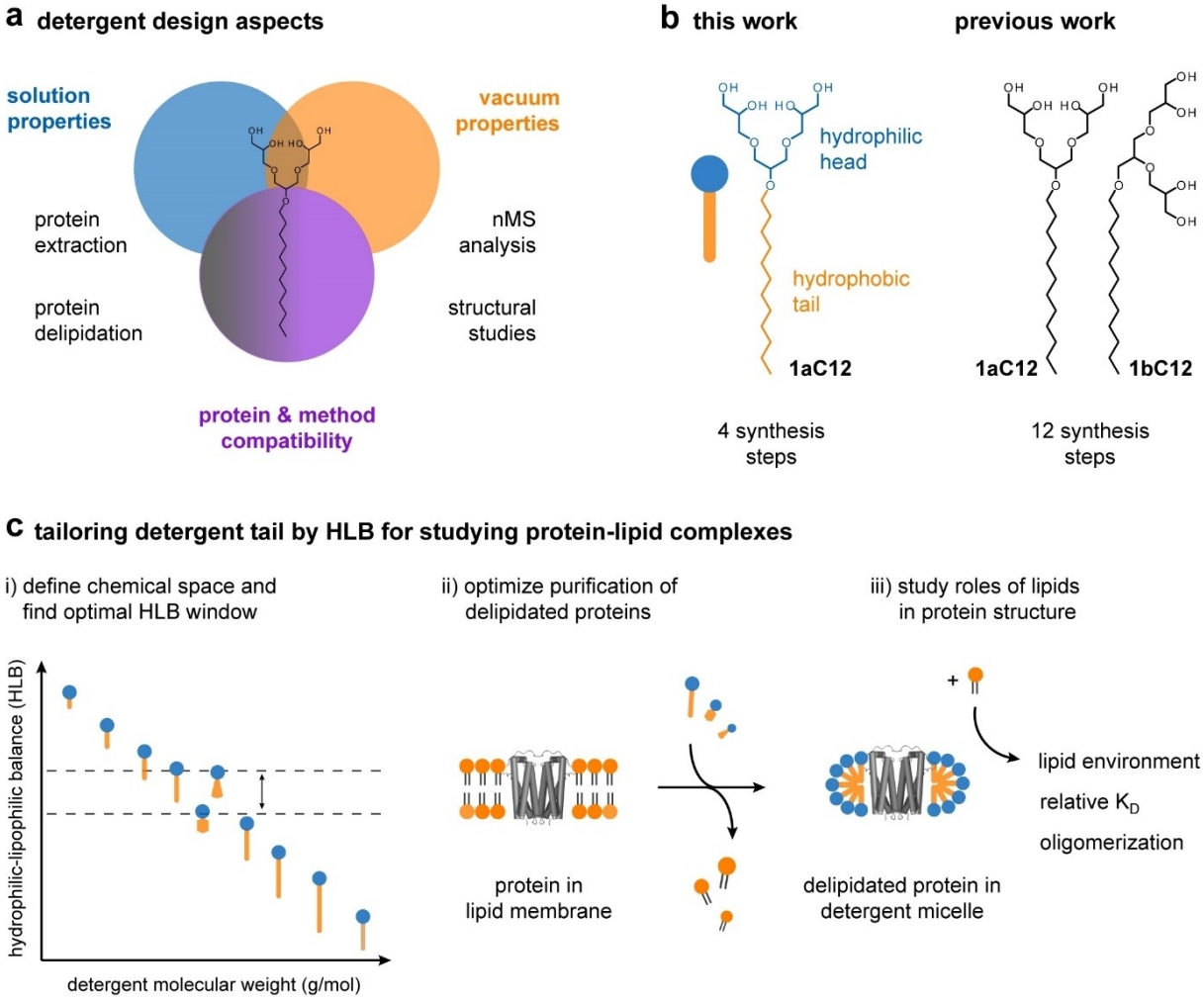

Figure 1. Overview about design, structure and optimization of [G1] OGDs for protein purification. a) Schematic showing detergent design aspects relevant for the purification and nMS analysis of membrane proteins. b) Structural overview about the individual [G1] OGD regioisomer **1aC12** that is subject of this study and the previously established [G1] OGD regioisomer mixture **1**. c) Schematic showing steps in the detergent selection tailored by HLB for improved purification of delipidated membrane proteins and nMS analysis of protein-lipid complexes. The HLB concept can be used to guide the optimization of detergents for the purification and analysis of membrane proteins.

A breakthrough came with the demonstration that the structure of oligoglycerol detergents (OGDs) can be predictably optimized for the nMS analysis of protein-lipid complexes (Figure 1b).[4] However, OGD design rules relate to specific OGD structures and are difficult to apply to other detergent classes.[17] To facilitate nMS of protein-lipid interactions, detergent design strategies are needed that are widely applicable among the detergentome (entirety of all detergents).

Detergents are widely used in membrane protein research and their utility is affected by the balance of their hydrophilic and hydrophobic groups.[17] Both facts inspired us to investigate the possibility that detergents can be optimized rationally by considering the hydrophilic-lipophilic balance (HLB) (Figure 1c). The HLB system introduced by Griffin in 1949 is used to compare the overall polarity of structurally different detergent classes based on numbers.[18] HLB values typically range from zero to 20 and are calculated from the molecular weight (MW) of the hydrophobic tail in relation to the MW of the detergent (Experimental Section). The lower the HLB value of a detergent, the lower is its overall polarity. HLB values facilitate the selection of detergents for applications in food and pharma industry,[19] for indexing cell surface properties of bacteria,[20] or for extracting membrane proteins from membranes.[17,21]

Here, we investigate the extent that detergents can be optimized for both the purification and delipidation of membrane proteins by means of the HLB system (Figure 1c). Compared to previous work on OGD regioisomer mixtures,[4,8,22] here we systematically investigate the role of the hydrophobic alkyl chain in individual [G1] OGD regioisomers for the ability to extract and delipidate membrane proteins (Figure 1b–c). Our results show that the HLB concept can be used to guide the structural optimization of the hydrophobic tail in detergents for the benefit of protein purification. We demonstrate that knowledge of delipidating properties of [G1] OGDs can be harnessed to study the lipid environment of membrane protein drug targets by nMS (Figure 1c).

Results and Discussion

Rational for a simplified [G1] OGD

OGD regioisomer mixtures were recently identified as innovative tools for membrane protein research (Figure 1b).[4,8,22] Heterogenous OGD regioisomer mixtures can provide a better mimic for heterogenous membranes compared to homogenous detergents and can extract large protein quantities from biological membranes.[4,22b] Furthermore, design guidelines were identified with which the molecular structure of OGDs can be optimized predictably for individual applications in membrane protein research, including protein extraction, delipidation, and nMS.[4] Availability of OGDs is key for mainstream adoption. However, OGD regioisomer mixtures are currently difficult to synthesize, as the synthesis procedure of a required starting material, for example, a specific oligoglycerol regioisomer mixture, has not yet been disclosed.[22b]

To facilitate mainstream adoption, here we investigate the utility of the individual [G1] OGD regioisomers as an alternative to [G1] OGD regioisomer mixtures. The [G1] OGD regioisomer **1 aC12** is a promising starting point for structure-property optimizations in membrane protein research. It is closely related structurally to the original [G1] OGD regioisomer mixture **1** (Figure 1b), facilitates the nMS analysis of membrane proteins, and can retain protein structure and function to a comparable level as the gold standard detergent *n*-dodecyl-β-D-maltoside (DDM).[22b,23]

To explore the potential of **1 aC12** for mainstream adoption, we first investigated the ease of its synthesis. The synthesis of [G1] OGD generally starts with the head group and is finalized by alkylation of the head group under basic conditions followed by removal of acetal protecting groups under acidic conditions (Experimental Section). The entire synthesis of **1 aC12** described here includes four steps (Figure 1b) (Supporting Information Figure S1). For comparison, since the starting material for the [G1] OGD regioisomer mixture **1** is not commercially available, both regioisomers **1 aC12** and **1 bC12** need to be synthesized separately. The entire synthesis of the [G1] OGD regioisomer mixture **1** includes 12 steps (Figure 1b) (Supporting Information Figure S1).

In summary, the individual [G1] OGD regioisomer **1 aC12** is currently easier to synthesize than the related [G1] OGD regioisomer mixture **1** and its starting material is widely available. Furthermore, **1 aC12** can be readily obtained from methallyl dichloride in four steps in multigram scale with high purity (> 96%) and an overall yield of 80%. Having established the synthesis of the individual [G1] OGD regioisomer **1 aC12**, we now evaluate its utility for the purification and analysis of membrane proteins.

Protein purification and delipidation

Establishing detergents is important for membrane protein research because it enables new protocols for the investigation of membrane protein structure and function.[3b,12a,c,24] Encouraged by the fact that bacterial membrane proteins can be targets for the development of new antibiotics,[25] we tested the general utility of **1 aC12** for purifying large quantities of bacterial membrane proteins by using GFP-tagged, tetrameric aquaporin (AqpZ-GFP) as a model system.[4] Following an established purification protocol,[4,26] we expressed AqpZ-GFP in *E. coli*, purified the protein in a detergent screen format by extraction and affinity purification, and compared relative protein quantities with the gold standard detergent DDM (Figure 2c). Similar relative protein quantities were obtained. This led us to the conclusion that the individual [G1] OGD regioisomer **1 aC12** is suitable for the extraction of large protein quantities from bacterial membranes.

To evaluate if **1 aC12** can preserve non-covalent protein-protein and protein-lipid interactions throughout purification, we applied nMS using a Q-Exactive UHMR mass spectrometer.[27] Mass spectra obtained following detergent removal in the vacuum of the mass spectrometer showed the expected oligomeric state of delipidated AqpZ-GFP and no lipid complexes were observed (Supporting Information Figure S2). This indicates that the individual [G1] OGD regioisomer **1 aC12** can retain the expected oligomeric state of a bacterial membrane protein and efficiently removes protein-lipid interactions throughout purification.[23] The properties of the [G1] OGD regioisomer **1 aC12** that led to the extraction and delipidation of large quantities of bacterial membrane proteins are similar to the characteristics of the [G1] OGD regioisomer mixture **1**.[4] This highlights the utility of the [G1] OGD regioisomer **1 aC12** as an alternative that is easier to synthesize than the [G1] OGD regioisomer mixture **1** (Figure 1b). We anticipate that the ease of the synthesis, availability of starting materials, and the utility for the purification and delipidation of large protein quantities will facilitate a mainstream adoption of the individual [G1] OGD regioisomer **1 aC12**.

Guiding OGD optimization by HLB

The ability to rationally design detergents is of considerable interest in membrane protein research.[4,11,12,17] During detergent purifications, membrane proteins become delipidated. Despite the fact that not all membrane proteins may tolerate delipidation without losing stability in solution,[28] the optimization of protein extraction and delipidation is important for at least two reasons: (1) Mildly delipidating detergents provide insights into lipid environments that co-purify with membrane proteins and, once lipid identity is confirmed, biological relevance can be studied.[3b] (2) Given that proteins remain stable after delipidation, strongly delipidating detergents can remove the lipidome, thus providing a source of lipid-free proteins for reconstitution into in vitro membrane environments to delineate the roles of lipids on protein structure and function.[3b] Previous reports showed that increasing the size of the OGD head group reduces delipidation but at the same time it reduces relative protein quantities.[4] Here, we focused on the role of the hydrophobic tail and investigated whether the HLB concept can be used to rationally guide the optimization of

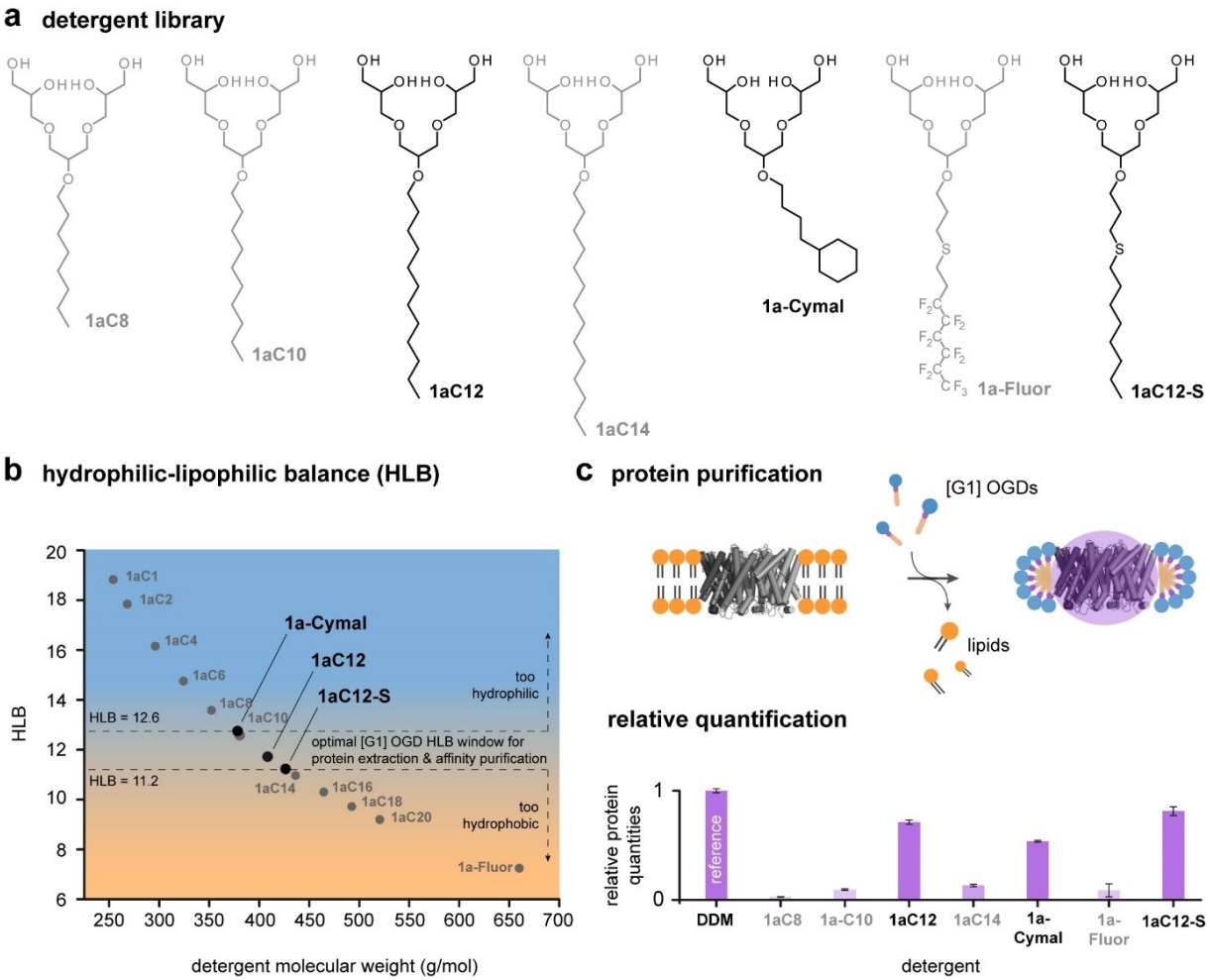

Figure 2. Exploring the optimization of the hydrophobic tail in [G1] OGDs by HLB. a) Schematic showing [G1] OGDs that are the subjects of the present study and differ in terms of the structure of the hydrophobic tail. b) HLB values of [G1] OGDs **1 aCm** with either **m** carbon atoms in the linear tail (**1 aC1**, **1 aC2**, …, **1 aC20**), a cyclohexane ring in the tail (**1 a-Cymal**), a fluorinated tail (**1 a-Fluor**), or a non-fluorinated analogue (**1 aC12-S**). c) Relative protein quantities obtained upon extraction and affinity purification of AqpZ-GFP with [G1] OGDs and the reference detergent DDM. Shifting the HLB values of [G1] OGDs to the HLB window of 11.2–12.6 by modifying their hydrophobic tail leads to improved relative protein quantities, as in the cases of **1 aC12**, **1 a-Cymal**, and **1 aC12-S**. Relative protein quantities were plotted with standard deviation ($n = 3$).

[G1] OGDs for the purification and delipidation of membrane proteins (Figure 1c).

To initiate the structural optimization, we defined a chemical space around the initial structure of the hydrophobic tail in **1 aC12** using our knowledge on OGDs (Figure 2a,b). It is intuitive to optimize protein extraction and delipidation by varying the number of carbon atoms in the linear, hydrophobic tail of detergents. In this regard, we defined [G1] OGDs that have between one and twenty carbon atoms in their linear, hydrophobic tail (Figure 2b). However, we expected that only [G1] OGDs with 8 to 14 carbon atoms in their hydrophobic tail will be suitable detergents, for example, **1 aC8**–**1 aC14**. From our experience, [G1] OGDs with a lower number of methylene groups in the tail will be too water-soluble to act as detergents, such as in the cases of **1 aC1**–**1 aC6** (Figure 2b). [G1] OGDs having a larger number of methylene groups in the tail will be poorly water-soluble, such as in the cases of **1 aC16**–**1 aC20** (Figure 2b).[29]

To identify optimal HLBs, we tested the utility of **1 aC8**, **1 aC10**, **1 aC12**, and **1 aC14** for the extraction of large quantities of AqpZ-GFP from bacterial membranes (Figure 2c). Higher protein quantities were obtained from **1 aC12** (Figure 2c). Control experiments with the translocator protein (*Rs*TSPO) and multidrug and toxin extrusion protein (*Pf*MATE) confirmed this finding (Supporting Information Figure S3). This indicates that varying the length of the linear hydrophobic tail in **1 aC12** in any direction reduces the ability to extract large protein quantities, regardless of the protein. The HLB value of **1 aC12** is about 11.7 and its utility to serve as a reference value for alternative optimization strategies was tested as discussed below.

To rationalize why **1 aC12** had the best performance among **1 aC8** to **1 aC14**, we hypothesized that varying the length of the linear hydrophobic tail in any direction reduces either the ability to solubilize membranes or to form stable proteomicelles.[17] To test this hypothesis, we decoupled the formation of proteomi-

celles from membrane solubilization. We performed this by preparing AqpZ and AmtB solubilized in DDM and then used size-exclusion chromatography (SEC) to exchange the detergent.[11] Protein precipitation occurred when DDM was exchanged for [G1] OGDs with shorter hydrophobic tails, for example, **1aC8** and **1aC10**. This indicates that lowering the number of methylene groups in the hydrophobic tail reduces the ability of [G1] OGDs to form stable proteomicelles which causes protein precipitation. nMS analysis of related samples confirmed the absence of target proteins in the supernatant since no signals of target proteins were obtained by nMS. In contrast, stable protein solutions were obtained when DDM was exchanged for [G1] OGDs with longer hydrophobic tails, for example, **1aC12** and **1aC14**. nMS experiments confirmed that the expected oligomeric state was retained during detergent exchange from DDM by SEC (Supporting Information Figure S4). Furthermore, signals of expected protein oligomers were also obtained by nMS upon extraction and affinity purification (Supporting Information Figures S5–S7). However, increasing the length of the hydrophobic tail in **1aC14** reduces its water-solubility (Supporting Information Table S1). Therefore, **1aC14** is less efficient in solubilizing membranes and reduced relative protein quantities are obtained upon extraction (Figure 2c). We conclude that the HLB value of **1aC12** of about 11.7 represents a sweet spot for the ability to obtain large relative protein quantities upon extraction and affinity purification.

An important question prompted by this study is whether it is possible to guide the structural optimization of the hydrophobic tail in [G1] OGDs by directing their HLB values closer to the HLB value of **1aC12**. To address this question, we synthesized the fluorinated version **1a-Fluor** with a HLB value of 7.2, far below the HLB value of **1aC12** (Figure 2b). The fluorinated detergent **1a-Fluor** is less soluble in water than **1aC12** and is likely too hydrophobic and fluorophilic to solubilize membranes.[12a,30] Therefore, lower relative protein quantities were obtained upon extraction (Figure 2c) (Supporting Information Figure S3). However, when the HLB of **1a-Fluor** was increased to 11.2 by exchanging its fluorine atoms for hydrogen atoms, such as in the case of **1aC12-S** (Figure 2a), higher relative protein quantities were obtained (Figure 2c). This indicates that shifting the HLB value of [G1] OGDs closer to the HLB of **1aC12** can be used to guide the optimization of the hydrophobic tail of a detergent for membrane protein purification. To probe the robustness of this approach, we optimized the structure of the hydrophobic tail in **1aC8**, which has an HLB value of 12.9 that lays above the HLB value of **1aC12** (Figure 2b). Reducing the HLB by extending the length of the tail by two carbon atoms will not produce a detergent that is suitable for protein extraction, such as in the case of **1aC10** (Figure 2c). Alternatively, we reduced the HLB of **1aC8** by introducing a cyclohexane ring (Figure 2a,b). Interestingly, the newly designed **1a-Cymal** can be used to purify moderate relative quantities of intact membrane proteins (Figure 2c) (Supporting Information Figure 3). Similar improvements of protein extraction performance have been obtained from the introduction of cycloalkanes into other detergents and amphiphilic polymers.[31] The relative protein quantities obtained from

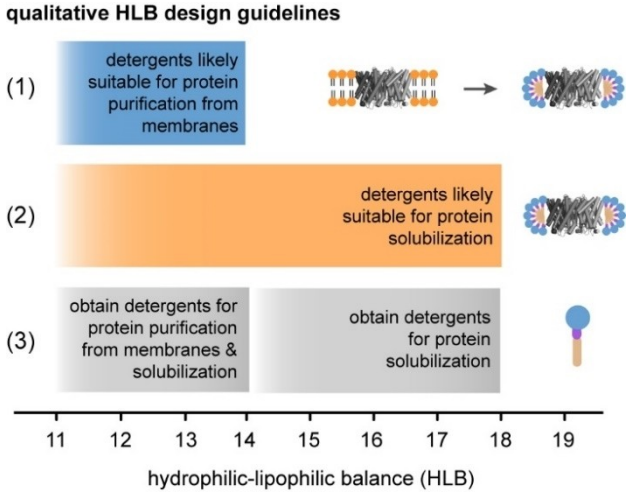

Figure 3. Qualitative HLB guidelines for streamlined detergent optimization. (1) Non-ionic detergents with HLB values between 11 and 14 are likely suitable for extraction and affinity purification of large protein quantities. (2) Non-ionic detergents with HLB values between 11 and 18 are likely suitable for protein solubilization. (3) Shifting HLBs of non-ionic detergents into the ranges defined in (1) and (2) enables likely the production of detergents that are suitable for protein purification from membranes and/or protein solubilization.

1a-Cymal were higher compared to those obtained from **1aC8**, **1aC10**, **1aC14**, and **1a-Fluor**. Even though the relative protein quantities obtained from **1a-Cymal** were not as high as those obtained from DDM, **1aC12**, and **1aC12-S**, membrane proteins can be readily purified in milligram quantities when the utilized detergent screen purification is upscaled by factor five or more. nMS experiments showed that the protein quantities obtained from individual preparations in the detergent screen obtained were sufficient for further analysis (~200 μg protein per detergent) (Supporting Information Figures S5–S7). Hence, although **1aC10** and **1a-Cymal** have similar HLB values they exhibit opposing utilities for membrane protein purification (Figure 2a,b). This led us to the conclusion that considering HLB values alone is not sufficient for optimizing the hydrophobic tail of [G1] OGDs. This is expected since the HLB value is calculated from the relative molecular weight of the hydrophobic tail (Experimental Section). The HLB system cannot be used to distinguish relative polarity differences in [G1] OGDs whose tails have similar molecular weights but differ in terms of branching and three-dimensional structure, such as in the cases of **1aC10** and **1a-Cymal** (Figure 1a). Furthermore, fluorinated detergents represent another boundary case since fluorinated alkyl chains are not only hydrophobic but also fluorophilic. Detergents with fluorinated alkyl chains commonly exhibit a lower miscibility with lipids than detergents containing hydrocarbon chains.[12a,30] As discussed above, this detail is not considered in our HLB calculations. However, once a detergent-class-specific, optimal HLB value has been identified, such as in the case of **1aC12** for [G1] OGDs, it is possible to guide the structural optimization of other [G1] OGDs by bringing their HLB values closer to that of **1aC12**.

More broadly, when aiming for the optimization of any detergent with a specific head group, available design strategies include atom exchange, lengthening, shortening, branching, or debranching of hydrophobic tails. While the utility of the individual design strategies has been demonstrated in numerous case studies,[12a,30,31c,32] a rational for choosing the best strategy to start with remains elusive. Therefore, it is common practice to evaluate all detergent design strategies regarding their utility for individual applications in membrane protein research. Subsequently, the best detergent design is understood retrospectively. Our data on [G1] OGDs indicate that the HLB concept serves as a framework for a streamlined selection of design strategies to enable the directed detergent optimization for the purification of large protein quantities from membranes.

In summary, our data outline strengths, and weaknesses of the HLB system for guiding the optimization of the hydrophobic tail in detergents for protein purification. In the cases of [G1] OGDs, the optimization of the hydrophobic tail guided by the HLB system led to the identification of new detergents that enable the extraction of large relative protein quantities from membranes, namely **1a-Cymal** and **1aC12-S** (Figure 2a–c). The final question left unanswered is whether it is also possible to optimize delipidating properties of [G1] OGDs following this approach. In this regard, nMS experiments revealed that [G1] OGDs exhibit strong delipidating properties, regardless of the hydrophobic tail (Supporting Information Figures S5–S7). Hence, the HLB system may not be used for guiding the optimization of hydrophobic tails in [G1] OGDs for tuning delipidation. Previous data revealed that increasing both the size of the head and branching of the hydrophobic tail in [G1] OGDs led to mildly delipidating, second-generation [G2] OGDs (Supporting Information Figure S8).[4] This agrees with the hypothesis that delipidating properties of detergents depend more on the chemical nature of the head group.[11] This leads us to the conclusion that (i) the structural optimization of the hydrophobic tail in [G1] OGDs guided by the HLB system enables their optimization for the purification of delipidated membrane proteins, while (ii) increasing both the size of the [G1] head and branching of the hydrophobic tail is necessary for efficiently modulating their delipidating properties.[4]

Qualitative HLB guidelines

Seen from a broader perspective, the term HLB has been used in the field of designing detergents for protein purification in two ways. More lately, for qualitatively stating that the utility of detergents is sensitive to the overall balance of polar and non-polar groups.[32c,33] Alternatively, as the metric that has initially been introduced by Griffin in 1949[18] and later being used to correlate protein purification outcomes with HLB numbers of detergents by Umbreit and Strominger.[21a] Subsequently, Storm et al. determined the HLB dependency for the solubilization of the plasma membrane-enriched fraction from rat liver with the Triton X-100 series.[34] Urner et al. further harnessed the use of the HLB metric for estimating the utility of non-ionic detergents for protein purification.[17,21b] Taken together, results obtained from Umbreit and Strominger,[21a] Storm et al.,[34] and Urner et al.[17] indicate that non-ionic detergents with HLB values between 12 and 14 are likely to enable the extraction and affinity purification of large protein quantities from membranes.

The HLB values of non-ionic [G1] OGDs that are suitable for the extraction and affinity purification of large protein quantities range from 11.2 to 12.6 (Figure 2b). This led us to the suggestion that the optimal HLB window derived from Umbreit et al., Storm et al., and Urner et al., i.e., 12 to 14, can be widened up to range from 11 to 14 (Figure 3). Interestingly, the HLB window ranging from 11 to 14 covers most non-ionic detergents that are relevant to membrane protein extraction and purification, including saccharide-, polyethylene glycol-, and oligoglycerol detergents (Supporting Information Table S2).[17,21b,34,35] However, we expect this HLB window to not cover all non-ionic detergents that are suitable for protein extraction and affinity purification. This relates to the fact that the HLB value is calculated from the relative molecular weight of the hydrophobic tail and does not give specific information about a detergent structure, which is a primary determining factor for a successful protein extraction and affinity purification. To sum up, the available knowledge about the utility of Griffin's HLB concept for designing detergents for membrane protein purification led us to the following qualitative detergent design guideline: (1) Non-ionic detergents with HLB values between 11 and 14 are likely to enable the extraction and affinity purification of large protein quantities from membranes (Figure 3).

Furthermore, detergents that do not enable the extraction and affinity purification of large protein quantities can still have value for membrane protein research. For example, detergents can also be used to solubilize membrane proteins upon detergent exchange. Since every detergent has individual pros and cons when it comes to protein purification and analysis, detergents are frequently exchanged.[21b,26] Therefore, expanding the pool of detergents that stabilize membrane proteins upon detergent exchange is as important as the identification of new detergents that enable extraction and affinity purification in one go.[17] In this regard, results from Youn et al. indicate that non-ionic detergents with HLBs between 11 and 13 can also solubilize membrane proteins upon detergent exchange.[36] Furthermore, results obtained from Urner et al. showed that non-ionic detergents with HLB values beyond 13.5 are likely more suitable for the solubilization of proteins upon detergent exchange than for protein extraction from membranes.[17] In the case of non-ionic detergents than can solubilize proteins, even higher HLB numbers were reported between 15 and 18, for example, for non-ionic hybrid-, Triton-, and Tween detergents.[17,21b,34,35,37] This led us to the following second, qualitative detergent design guideline: (2) Non-ionic detergents with HLB values between 11 and 18 are likely to enable the solubilization of membrane proteins upon detergent exchange and in the absence of membranes (Figure 3).

However, the selection of hydrophobic tails that leads to [G1] OGDs that are suitable for the extraction and affinity purification of proteins or the solubilization of proteins upon

detergent exchange is much smaller than the selection of all possible hydrophobic tails (Figure 2c). Furthermore, the detergent-class-specific, optimal HLB window identified for [G1] OGDs lays between 11.2 and 12.6 and is narrower than the optimal HLB windows discussed above in (1) and (2) (Figure 3). This is expected, because the optimal HLB window of non-ionic detergents is not only determined by the structure of the hydrophobic tail but also by the structure of the hydrophilic head group.[17,21] This led us to the suggestion that every detergent class has an individual optimal HLB window that needs to be identified empirically. Finally, this led us to the third, qualitative detergent design guideline: (3) Modifying the hydrophobic tail within a detergent class to shift HLB values towards a detergent-class-specific, optimal HLB window, i.e., 11.2 to 12.6 in the case of [G1] OGDs, can lead to the obtainment of new detergents. Given that the empirically determined and detergent-class-specific, optimal HLB windows overlaps with the HLB window defined in (1) above, i.e., between 11 and 14, then new detergents are likely to enable the purification of large protein quantities from biological membranes (Figure 3). Given that the empirically determined and detergent-class-specific, optimal HLB windows overlaps with the HLB window defined in (2) above, i.e., between 11 and 18, then new detergents are likely to solubilize membrane proteins upon detergent exchange (Figure 3). We anticipate the qualitative HLB guidelines will direct us closer to a streamlined optimization of detergents for applications in membrane protein research.

Bacterial protein-lipid interactions

Detergents and nMS enable the investigation of membrane protein structure in response to interactions with small molecules.[14a,38] From our experience, the heterogeneity and adhesiveness of native membranes can hamper a direct nMS analysis of these interactions.[4,14a,b] Therefore, mildly delipidating detergents are used to reduce the heterogeneity of protein-lipid complexes during purification to a level that their interactions can be analyzed by nMS.[4] Strongly delipidating detergents are used to remove practically all the native lipids that co-purify with membrane proteins. Provided that target proteins remain stable after delipidation, individual lipids can be added selectively, which can enable studying their roles in protein structure and function.[2a,b,3b,14a,39] In this way, detergents and nMS facilitate the investigation of the role of lipids for protein structure and function,[2] relative strength of individual protein-lipid interactions,[2c,40] protein-lipid stoichiometries,[41] and allosteric effects in lipid and drug binding.[2c,42] However, detergents that provide sufficient delipidation without destabilizing protein complexes are often hard to find.[4]

To establish the utility of the best performing [G1] OGD regioisomer **1aC12** for the investigation of protein-lipid interactions by nMS, we focused on the bacterial ABC transporter BtuCD from E. coli. ABC transporters are drug targets that mediate the transport of small molecules through membranes.[43] Previous data showed that BtuCD co-purifies with phospholipids (PLs).[44] However, complete delipidation has not yet been achieved,[44] thereby hampering a complete analysis of BtuCD-PL interactions. Due to its ability to delipidate and stabilize bacterial proteins, **1aC12** enabled the facile nMS analysis of fully delipidated BtuCD (Figure 4a). This enabled us to determine relative dissociation constants (K_D values) for individual PLs by nMS, including cardiolipin (CDL), phosphatidylglycerol (PG), and phosphatidylethanolamine (PE), which are the main PL components of E. coli membranes (Figure 4b). Lower relative K_D values were obtained from CDL and PG (Figure 4b). Lipid concentrations required to determine a relative K_D for PE were impractical for nMS ($>40\,\mu M$). This indicates that BtuCD binds more strongly to CDL and PG in membranes compared to PE (Figure 4b). In summary, **1aC12** can stabilize delipidated proteins and enables the nMS analysis of protein-lipid complexes after adding lipids back to delipidated proteins.

The ability to determine relative K_D values can help to estimate the transient nature of protein-lipid interactions in membrane environments.[2c,45] This approach can require complete protein delipidation in the first step, which can change the oligomeric states of membrane protein.[46] To investigate the utility of **1aC12** for exploring the impact of delipidation on protein oligomerization, we focused on the dimeric ABC transporter MacB from E. coli.[47] Using nMS, Barrera and co-workers found that MacB co-purifies with a ligand whose mass matches with the membrane lipid PE.[48] To systematically study the effect of all PLs on oligomerization in vitro, we first analyzed MacB by nMS upon extraction, affinity purification, and delipidation with **1aC12**. nMS data revealed a delipidated oligomer equilibrium in **1aC12** consisting of 27% delipidated MacB monomer and 73% delipidated MacB dimer (Figure 4c,d) (Supporting Information Table S4). Interestingly, MacB dimers form the functional component of a MacAB/TolC drug efflux pump whose activity is strongly linked to conferring resistance to macrolide antibiotics.[49] To evaluate the extent that the monomer-dimer equilibrium of MacB is affected by delipidation, we ran control experiments with the mildly delipidating detergent DDM. nMS data obtained following purification and analysis under comparable instrument conditions revealed mainly MacB dimers in complex with small ligands (Figure 4c,d) (Supporting Information Table S3). The ligand masses agreed with those of CDL or dimers of lower MW PLs (Supporting Information Table S3). Inspired by an established procedure,[2b,14b] we evaluated whether the oligomer equilibrium is affected by these lipids by titrating individual PLs back to fully delipidated MacB in **1aC12**. nMS analysis revealed that adding individual PL classes back to delipidated MacB in **1aC12** shifts the oligomer equilibrium from MacB monomers towards MacB dimers to varying degrees (Supporting Information Table S4). MacB dimerization in **1aC12** was most pronounced in the presence of CDL and PE (Supporting Information Table S4). This indicates that CDL, PE, and PG support the formation of MacB dimers in membranes to varying degrees. Our data indicate that **1aC12** enables the nMS analysis of membrane protein oligomerization in response to lipids.

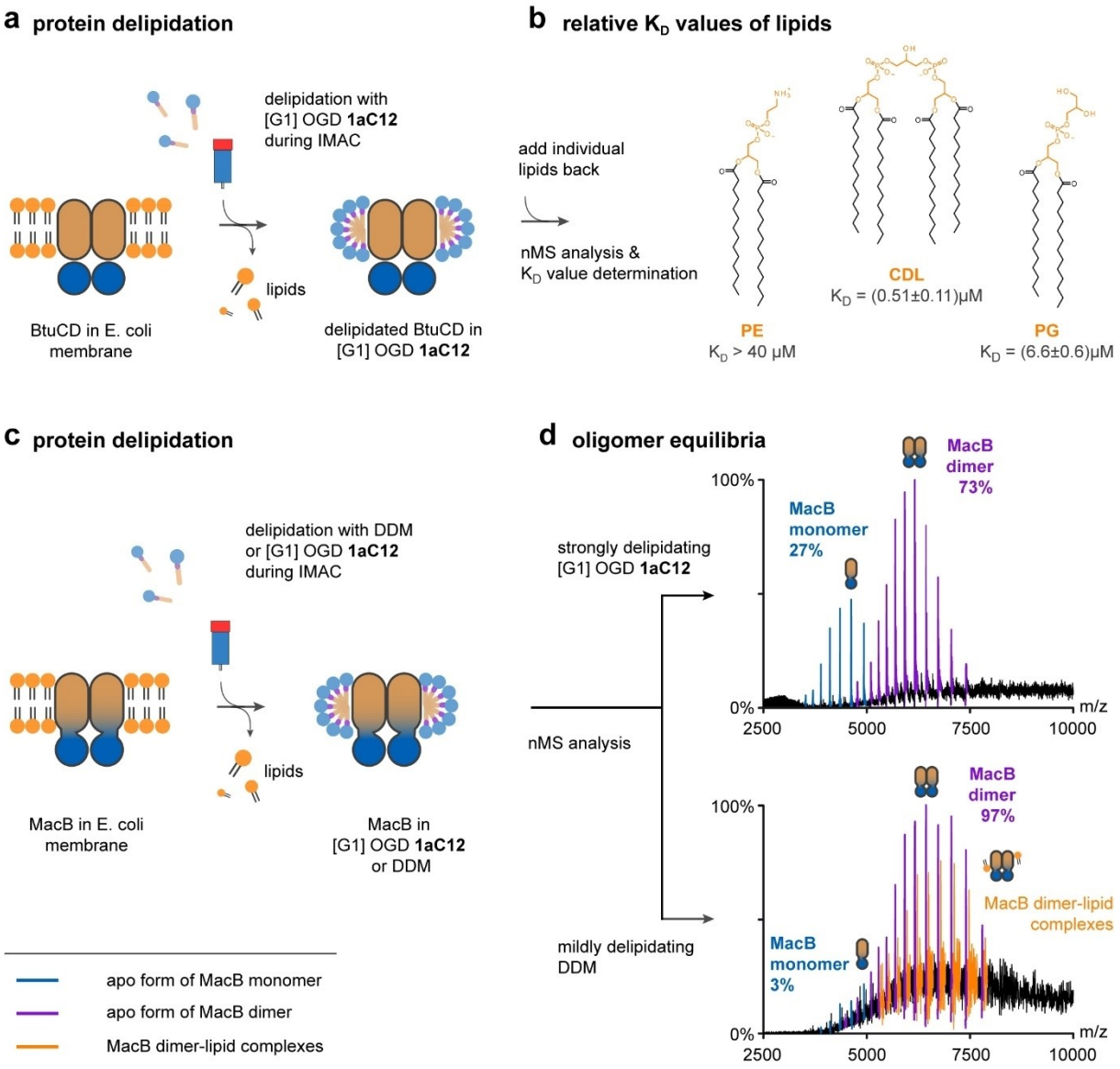

Figure 4. Studying the role of lipids for bacterial protein structures with [G1] OGD **1aC12** and nMS. a, b) Schematic showing the steps involved in the purification of delipidated BtuCD and the determination of K_D values for individual phospholipids (PLs) by nMS. The individual [G1] OGD regioisomer **1aC12** enables the determination of relative K_D values for protein-lipid complexes by nMS that are added back to delipidated membrane proteins. c, d) Schematic showing steps involved in assessing the role of lipids for membrane protein oligomerization by means of detergents and nMS. nMS data obtained upon purification with strongly delipidating **1aC12** and mildly delipidating DDM show that the MacB monomer-dimer equilibrium is sensitive to the co-purification of lipids. Mass spectra were acquired using similar instrument conditions.

Detergents exhibit individual utilities for the purification of membrane protein-lipid complexes and their analysis by nMS.[4,11] Compared to mildly delipidating DDM, the detergents C8E4 and LDAO are commonly used to delipidate membrane proteins and to analyze protein-lipid complexes by nMS after titrating lipids back.[2a,c,45] Lower activation energies are required for the liberation of membrane proteins from their micelles inside a mass spectrometer.[11] Furthermore, both detergents efficiently reduce the number of charges attached to membrane proteins in the gas-phase.[11]

Both parameters help to maintain non-covalent protein-protein and protein-lipid interactions in the gas-phase.[50] However, nMS results obtained from C8E4 and LDAO are not directly comparable with DDM. DDM exhibits mildly delipidating properties but does not reduce the charge of membrane proteins under comparable instrument conditions.[4,11,22a] The activation energy experienced by protein ions is proportional to their charge and more activation energy is usually required for sufficient detergent removal with DDM.[11] Therefore, harsher activation conditions are required inside the mass spectrometer to obtain nMS data from membrane proteins solubilized in DDM compared to C8E4 and LDAO, which can bias relative intensities of oligomers and protein-lipid complexes.[11] This commonly leads to the question as to whether relative

intensities of oligomers and protein-lipid complexes obtained from these detergents are due to their stabilization in solution or gas-phase.[4] Here we show that **1aC12** can help to circumvent this problem. Indeed, like C8E4 and LDAO, **1aC12** exhibits strong delipidating properties.[4] In contrast, **1aC12** acts like DDM in terms of charge reduction as it does not reduce the charge of membrane protein ions.[4] Overall, since **1aC12** and DDM exhibit opposing delipidating properties in solution and similar charge-reducing properties in the gas phase, the comparison of nMS data obtained using these two detergents can directly inform on the role of lipids for membrane protein structures under the experimental conditions employed.

Conclusion

In summary, we established the utility of the individual [G1] OGD regioisomer **1aC12** for membrane protein extraction, delipidation, and studying protein-lipid interactions by nMS. Advantages of detergent **1aC12** include i) the ease and feasibility of its synthesis compared to previously established and heterogenous OGD detergent regioisomer mixtures, ii) the ability to extract and delipidate large relative protein quantities from bacterial membranes, and iii) the ease of the nMS analysis of protein-lipid interactions after titrating lipids back to delipidated proteins. [G1] OGD **1aC12** is a suitable addition to the repertoire of detergents in the field and enables the analysis of relative K_D values of protein-ligand complexes and oligomer equilibria in response to ligand binding in vitro.

More broadly, our results underline that the utility of detergents to purify large protein quantities from biological membranes is sensitive to the structure of the hydrophobic tail. Our data indicate that if the hydrophobic tail is too short, the detergent's ability to stabilize membrane proteins is reduced. Furthermore, if the hydrophobic tail is too long, the detergent's ability to solubilize membranes is reduced. Among the different combinations of the [G1] head group and various hydrophobic tails tested, [G1] OGD **1aC12** turned out to be a sweet spot for maintaining protein stability and at the same time enabling the solubilization of membranes.

Moreover, we found that the Griffin's HLB system can be used to guide the structural optimization of the hydrophobic tail in detergents. For this purpose, we propose two detergent design guidelines, i.e., (1) A non-ionic detergent with a HLB value between 11 and 14 is likely to enable the purification of large protein quantities from membranes through extraction and affinity purification; (2) A non-ionic detergent with a HLB values between 11 and 18 is likely to stabilize proteins upon detergent exchange. However, since the HLB of detergents is not only determined by the structure of the hydrophobic tail but also by the structure of the hydrophilic head group, we also conclude that every detergent class has an individual optimal HLB window. Finally, this led us to propose a third, qualitative detergent design guideline: (3) Shifting the HLB of a non-ionic detergent with a specific head group towards a detergent-class-specific, optimal HLB window by modifying its hydrophobic tail can lead to new detergents that are suitable for the extraction and/or solubilization of membrane proteins. In the case of [G1] OGDs, the detergent-class-specific, optimal HLB window ranges from 11.2 to 12.6 under the experimental conditions employed. Following this idea, we modified the hydrophobic tail in [G1] OGDs accordingly and identified new detergents that enable the purification of bacterial membrane proteins. Furthermore, we found that [G1] OGDs exhibit strong delipidating properties, regardless of the hydrophobic tail. The latter result confirms the long-standing hypothesis that delipidating properties of detergents depend more on the structure of the detergent head group than on the hydrophobic tail. We anticipate that HLB guidelines will facilitate the delivery of new detergent tools for the analysis of challenging drug targets.

Experimental Section

Starting materials for detergent synthesis: 1-Bromohexane, 1-bromooctane, 1-bromodecane, allyl bromide, AIBN, [15]-crown-5 and 1H,1H,2H,2H perfluorooctanethiol were purchased from Sigma Aldrich. [18]-Crown-6, 1-bromododecane, 1-bromotetradecane, and dry DMF over molecular sieve were purchased from Acros Organics. Hydrochloric acid (37 w%) was purchased from Fisher Scientific. Octanethiol was purchased from Alfa Aesar. (4-Bromobutyl)-cyclohexane was purchased from Life Chemicals. The symmetric regioisomer of acetal-protected, triglycerol [pG1]-OH was synthesized as described before.[4,51] All solvents and reagents were used as supplied. Ethyl acetate was distilled and azobisisobutyronitrile was recrystallized prior to use. Methanol and deionized water were degassed before their use as HPLC eluent. For all reactions requiring inert conditions argon was used as inert gas. The symmetric [pG1]-OH regioisomer was purified with HPLC using *n*-hexane/isopropanol, 4/1 *v*/*v*, as the eluent.

Chromatography and detergent characterization: For thin-layer chromatography (TLC), sheets of ALUGRAM Xtra SIL G/UV254 with a 0.20 mm layer of silica 60 from Macherey-Nagel were used. TLC plates were stained with cerium sulphate/ molybdic acid solution [cerium(II) sulphate (10 g), molybdic acid (25 g), sulfuric acid (60 mL), water (940 mL)]. For normal-phase chromatography purifications, silica gel 60 (0.040–0.063 mm) from Macherey-Nagel was used. For preparative reversed-phase (RP)-HPLC purification of deprotected detergents, a HPLC-system containing a Shimadzu CBM-20A controller, a dual Shimadzu, LC-8A pump, a Knauer variable wavelength monitor (64 series) RI detector, a Knauer UV-detector and a Rheodyn injector with a sample volume of 10 mL was used. The system was run with a RP-18 column (RSC-gel, C18ec, 5 µm, 250 mm × 32 mm) from RSC with a flow rate of 40 mL/min. Analytical RP-HPLCs were performed with a Knauer Smartline system containing a dual pump 1000 with degasser, an automatic sampler 3950, a RI detector and an UV-Detektor 2500. The system was run with a RP 18 column (RSC-gel, C18ec, 5 µm, 250 mm × 4 mm) from RSC with a flow rate of 1 mL/min. To confirm the molecular structures of the detergents, NMR spectra were recorded on an ECX400 from JEOL (400 MHz), an ECZ600 (600 MHz) from JEOL and an AVANCE700 from Bruker (700 MHz). Mass spectra for detergents and detergent precursors were measured by the core facility Biosupramol with an Agilent 6210 mass spectrometer in high resolution mode.

Detergent synthesis

General procedure for the alkylation of [pG1]-OH under SN2 conditions: Symmetric, acetal-protected triglycerol [pG1]-OH (1–4 g) was dissolved in a round-bottom flask with dry DMF (90 mL) under argon atmosphere. The round-bottom flask was put into an ice bath and the mixture was stirred for 5 min. Subsequently, sodium hydride (60 w% suspension, stabilized with mineral oil, 6 equiv.) was added in small portions. The ice bath was removed, and the mixture was allowed to warm up to room temperature (~22.5 °C) over a period of 60 min. The desired bromoalkane (6 equiv.) was added dropwise. The mixture was stirred for a minimum of 9 h at 80 °C. The mixture was cooled with an ice bath and water was added dropwise (20 mL). The solvent was removed under reduced pressure. The remaining residue was suspended in water (100 mL) and brine (100 mL). The aqueous layer was extracted with ethyl acetate (3×100 mL). The combined organic layers were dried over sodium sulfate. The solvent was removed under reduced pressure. Column chromatography (SiO_2, n-pentane/ethyl acetate) gave the desired acetal-protected precursors for **1aC8**, **1aC10**, **1aC12**, **1aC14**, and **1a-Cymal** in good yields (54% – quant). Details about the synthesis of individual alkylation products, including NMR and MS characterization, are provided for download in the Electronic Supporting Information.

Procedure for the allylation of [pG1]-OH under SN2' conditions: [pG1]-OH (12.0 g, 37.4 mmol) and catalytic amounts of [15]-crown-5 were dissolved in dry tetrahydrofurane (300 mL). Sodium hydride (60 w% suspension, stabilized with mineral oil, 5.94 g, 149 mmol) was added in small portions and the mixture was stirred for 2 h at 40 °C. Allyl bromide (6.50 mL, 9.10 g, 75.2 mmol), catalytic amounts of [18]-crown-6, and catalytic amounts of potassium iodide were added and the mixture was stirred at 65 °C for 18 h. The mixture was cooled with an ice bath and water (30 mL) was added slowly. The solvent was removed under reduced pressure. The residue was suspended with water (170 mL) and dichoromethane (200 mL). The aqueous layer was extracted with dichloromethane (3× 200 mL). The organic layer was washed with brine (100 mL) and dried over sodium sulfate. The solvent was removed under reduced pressure. Filtration over silica (SiO_2, *n*-pentane/ethyl acetate, 50/1 *v/v*→4/1) gave the desired product [pG1] allyl ether (12.7 g, 35.3 mmol, 94%). Details about NMR and MS characterization are provided in the Electronic Supporting Information for download.

Procedure for thiol-ene reaction with fluorinated tail: [pG1] allyl ether (5.85 g, 16.2 mmol) was dissolved in 1H,1H,2H,2H-perfluorooctanethiol (15 g, 39.5 mmol) and argon was bubbled through the solution for 15 min. The solution was further degassed via freeze-pump-thaw cycling and was subsequently heated up to 80 °C under argon atmosphere. A spatula tip full of azobisisobutyronitrile was added and the mixture was stirred for 2 h at 80 °C. Subsequently, an additional spatula tip full of azobisisobutyronitrile was added and the mixture was stirred for 16 h at 80 °C. Subsequently, an additional spatula tip full of azobisisobutyronitrile was added and the mixture was stirred for 4 h at 80 °C. The solution was then concentrated under reduced pressure and subsequent filtration over silica gel (SiO_2, *n*-pentane/ethyl acetate, 25/1 *v/v*→4/1) gave the acetal-protected precursor for **1a-Fluor** (8.20 g, 11.1 mmol, 69%). Details about NMR and MS characterization are provided in the Electronic Supporting Information for download.

Procedure for thiol-ene reaction with hydrocarbon tail: [pG1] allyl ether (6.85 g, 19.0 mmol) was dissolved in octanethiol (15.0 mL, 12.6 g, 86.1 mmol) and argon was bubbled through the solution. The solution was further degassed via freeze-pump-thaw cycling and was heated up to 80 °C. A spatula tip full of azobisisobutyronitrile was added and the mixture was stirred for 2 h at 80 °C. Subsequently, an additional spatula tip full of azobisisobutyronitrile was added and the mixture was stirred for 16 h at 80 °C. Subsequently, an additional spatula tip full of azobisisobutyronitrile was added and the mixture was stirred for 4 h at 80 °C. The solution was concentrated under reduced pressure and subsequent filtration over silica gel (SiO_2, n-pentane/ethyl acetate, 25/1 *v/v*→4/1) gave the acetal-protected precursor for **1aC12-S** (9.17 g, 18.1 mmol, 95%). Details about NMR and MS characterization are provided in the Electronic Supporting Information for download.

General procedure for acetal deprotection: Acetal-protected detergents (2–10 g) were dissolved in methanol (800 mL), hydrochloric acid (37%, 100 μL) was added, the mixture was stirred at room temperature (~22.5 °C) for 8–24 h and the solvent was removed under reduced pressure. The remaining residue was dissolved again in methanol (800 mL), hydrochloric acid (37%, 100 μL) was added, the mixture was stirred at room temperature (~22.5 °C) for 8–24 h and the solvent was removed under reduced pressure. Purification through RP-HPLC (methanol/water, isocratic) gave the desired products **1aC8**, **1aC10**, **1aC12**, **1aC14**, **1a-Cymal**, **1a-Fluor**, and **1aC12-S**. Details about utilized solvent mixtures for RP-HPLC, NMR, and MS characterization of individual detergents are provided in the Electronic Supporting Information for download.

Dynamic light scattering: Critical aggregation concentration (cac) values were determined by means of dynamic light scattering following an previously optimized procedure:[4,8,21b] Briefly, dilution series with detergent concentrations between 10^{-8} and 10^{-2} mol L^{-1} were prepared in ultrapure water, which was obtained from a Milli-Q system (18.2 MΩ cm). All samples were filtered (0.22 μm, RC) and equilibrated for at least 16 h at room temperature (approximately 22 °C) prior analysis. The samples were analysed in cuvettes (Quartz Suprasil, width× length: 2 mm×10 mm) using a Zetasizer Nano-ZS ZEN3600 (Malvern, UK). The instrumental parameters were as follows: material (polystyrene latex), dispersant (water), sample viscosity parameters (use dispersant viscosity as sample viscosity), temperature (22.5 °C), equilibration time (120 s), cell type (quartz cuvettes), measurement angle (173° backscatter), measurement duration (manual), number of runs (11), run duration (10 s), number of measurements (3), delay between the measurements (0 s), data processing (general purpose, normal resolution). The derived count rate values obtained from three

measurements per concentration were averaged. The unit of the derived count rate is kilo counts per second (kcps). The logarithm of the derived count rate was plotted against the logarithm of the concentration. The double logarithmic plots showed two characteristic regions: 1.) a flat region with low count rates at lower detergent concentrations and 2.) a linear growth of the count rate at higher concentrations. Both regions were fitted to linear functions and the intersection was taken as the *cac* value. The cac values are summarized in Supporting Information Table S5.

Hydrophilic-lipophilic balance: The hydrophilic-lipophilic balance (HLB) of our detergents was calculated using Griffin's equation[18] shown in equation below in which individual parameters are defined as follows: molecular weight of the tail (MW_{tail}) and molecular weight of the detergent (MW). HLB values are summarized in Supporting Information Table S1 and S2.

$$HLB = 20 \times \left(1 - \frac{MW_{tail}}{MW}\right)$$

Membrane protein purification: Membrane proteins described throughout this study were expressed and purified with DDM, **1aC8**-**1aC14**, **1aC12-S**, **1a-Cymal**, and **1a-Fluor** as outlined in detail in Ref. [26] For details on expression, membrane preparation, extraction and affinity purification see the step-by-step protocol described in Ref. [26]. Protein parameters for *E. coli* AqpZ-GFP, *Pf*MATE-GFP, and *Rs*TSPO are summarized in Supporting Information Table S4, including monomer molecular weight, secondary structure, and number of transmembrane helices.

To purify MacB, the same procedure described in Ref. [26] was used, but the expression plasmid has been prepared as follows: a gene encoding MacB was synthesized by IDT and cloned into a modified pet28 vector using In-Fusion Cloning (Takara) which encodes for an N-terminal hexahistidine tag separated from the gene by a linker (thrombin and TEV cleavage motifs). Furthermore, in the case of MacB, purification buffers have been changed from Tris to HEPES. Expression and membrane preparation for MacB has been done as described below:

The MacB plasmid was transformed into *E. cloni* EXPRESS BL21(DE3) Chemically Competent Cells (1 μL plasmid solution into 50 μL cells, kanamycin resistance). Three colonies were transferred from agar plate into LB Broth medium (5 mL, 50 μg/mL kanamycin). The cell suspensions were shaken with 180 rpm at 37 °C for 19 h and then added to LB Broth medium (2× 200 mL, 50 μg/mL kanamycin). The cell suspensions were shaken with 180 rpm at 37 °C for 9 h. LB Broth medium (12×1 L, 50 μg/mL kanamycin) was inoculated with cell suspensions (30 mL per 1 L LB Broth). The mixtures were shaken with 180 rpm at 29 °C for 13 h. Protein expression was induced by adding IPTG (1 mL of a 1.54 M aqueous solution per 1 L LB Broth). The cell suspensions were shaken with 180 rpm at 28 °C for 2.5–3 h. Cells were harvested by centrifugation (5,000 g× 10 min). Supernatants were discarded and cells were suspended in buffer (150 mL of 100 mM HEPES, 400 mM NaCl, 30% *v/v* glycerol, 3 protease inhibitor tablets, pH = 7.5). Cells were lysed using a Microfluidizer (1,500 bar, 4 °C). The supernatant was clarified by centrifugation (20,000 g, 20 min, 4 °C) and isolated. Membrane fractions were pelleted from the isolated supernatant by ultracentrifugation (125,000–175,000 g, 45 min, 4 °C). The supernatant was discarded, and the pelleted membranes were suspended in buffer (6 mL of 100 mM HEPES, 400 mM NaCl, 30% *v/v* glycerol, 1 protease inhibitor tablet per 50 mL, pH = 7.5). Suspended membranes were divided into 2 mL aliquots, flash frozen in liquid nitrogen and stored at −80 °C for up to two years prior to use.

To purify MacB through extraction and affinity purification, suspended membranes were thawed on ice. Extraction and affinity purification of MacB has been done as follows: An aliquot of MacB-containing membrane suspension (200 μL) was mixed with detergent-free suspension buffer (700 μL of 100 mM HEPES, 400 mM NaCl, 30% glycerol, 1 protease inhibitor tablet per 50 mL, pH = 7.5), and detergent stock solution (100 μL of a 10 w% *w/v* solution of DDM or **1aC12**). The mixture was agitated for 10 min at 4 °C. The supernatant was isolated by centrifugation (10,000×*g*, 10 min, 4 °C) and purified by IMAC. An empty spin column (1.2 mL, Bio-Rad) was loaded with Ni-Agarose suspension (600 μL, Quiagen). The column was washed with IMAC wash buffer (500 μL, 25 mM HEPES, 200 mM NaCl, 25 mM imidazole, 10% *v/v* glycerol, 2×cac DDM or **1aC12**, pH = 7.5). The column was loaded with MacB-containing, clarified supernatant, washed with IMAC wash buffer (5× 500 μL, 2×cac DDM or **1aC12**) and an IMAC buffer mixture (1000 μL of wash/elution buffer, 9/1 *v/v*, 2×cac DDM or **1aC12**). Proteins were eluted with IMAC elution buffer (500 μL of 25 mM HEPES, 200 mM NaCl, 350 mM imidazole, 10% *v/v* glycerol, 2× cac DDM or **1aC12**, pH = 7.5). Freshly eluted protein solutions were concentrated to a volume of 70 μL in Amicon Ultra 0.5 mL centrifugal filters (MWCO = 100 kDa, 13,500 g×6 min, 4 °C). The protein concentration was calculated from the absorbance at 280 nm by using the molecular extinction coefficient (66475 $M^{-1}cm^{-1}$) that was calculated from the following amino acid sequence provided in the Electronic Supporting Information.

Furthermore, the other membrane proteins AqpZ-GFP, *Pf*MATE-GFP, and *Rs*TSPO were purified following the same procedure but with detergent-containing Tris buffers.[26] Relative protein quantities were determined by UV/VIS spectroscopy, normalized to DDM and plotted against the detergent abbreviation with standard deviation from three independent repeats ($n = 3$) (Figure 2c) (Supporting Information Figure S3).

Native mass spectrometry: To monitor protein identity, oligomeric state, and delipidation, a 10 μL aliquot of membrane protein solution obtained upon IMAC was transfered into detergent-containing mass spectrometry buffer (200 mM ammonium acetate and 2×cac detergent) via centrifugal buffer exchange over two 75 μL Zeba™ Spin Desalting Columns (MWCO = 7 kDa, Thermo Fisher Scientific). The protein solution was analysed using a modified Q Exactive MS instrument using the following experimental parameters: injection flatapole (7.9 V), inter flatapole lens (6.9 V), bent flatapole (5.9 V), transfer multipole (4 V), capillary voltage (1.2 kV), source temperature

(100 °C), voltage applied to the C-trap entrance lens (5.8 V), in-source trapping voltage (100 V), higher-energy collisional dissociation (HCD) cell voltage (300 V), HCD cell pressure (9×10^{-10} mBar), noise level parameter (3), microscans (10), and resolution (9,000). Mass spectra data (ion intensity vs m/z) were exported and plotted with OriginPro 9.1. Mass spectra then were exported as Adobe Illustrator files, processed with Adobe Illustrator, and exported as JPG files (Figure 4) (Supporting Information Figures S4–S8).

Relative K_D values of BtuCD-lipid complexes: BtuCD was expressed as described before[44] and purified with [G1] OGD **1aC12** during extraction and affinity purification to obtain its delipidated form. For the determination of relative K_D values of lipids, BtuCD purified in [G1] OGD **1aC12** micelles was incubated with either 1,2-dimyristoyl-*sn*-glycero-3-phosphoethanolamine (14:0/14:0 PE, DMPE), 1,2-dimyristoyl-*sn*-glycero-3-phosphorylglycerol sodium salt (14::0/14:0 PG, DMPG), or 14:0 CDL to obtain a final protein concentration of 5 μM. PE was tested at 40 μM final concentration. PG binding was assessed at the following final lipid concentrations: 2.5, 5, 10, 20, and 40 μM. CDL binding was assessed at the following final lipid concentrations: 0.3125, 0.625, 1.25, 2.5, 5, 10, and 20 μM. Sample buffer also contained ammonium acetate (200 mM) and [G1] OGD **1aC12** (2×cac). Samples were incubated on ice for 10 min and were subsequently analysed by nMS as described above with the following modifications: negative polarity; capillary voltage (0.9 kV), source temperature (200 °C), in-source trapping voltage (0 V), microscans (5), resolution (17,500). Peak intensities were then extracted and the ratios of the intensity of the lipid bound peak versus the total intensity of all observed species were calculated. Average and standard deviation values of these ratio states from three independent experiments were plotted against lipid concentration. The data were fitted globally using GraphPad Prism 8.0 with the equation:

$$y = \frac{B_{max} \cdot x}{x + K_D}$$

where x refers to protein concentration, y is the fractional abundance of protein-lipid species, and B_{max} is the maximum specific binding, in the same units as y.

Relipidation of MacB: Delipidated MacB purified in [G1] OGD **1aC12** micelles was incubated with either PE, PG, or CDL to obtain a final protein concentration of 1 μM and final lipid concentrations of 3 μM. Sample buffer also contained ammonium acetate (200 mM) and [G1] OGD **1aC12** (2×cac). Samples were incubated on ice for 2 min and were subsequently analysed by nMS as described above. Oligomer equilibria are summarized in Supporting Information Table S3.

Acknowledgements

K. Pagel, I. Liko, J. Gault, J. R. Bolla, V. Wycisk, D. Rauh, and the Core Facility BioSupraMol of the Freie Universität Berlin are gratefully acknowledged for continuous support. T.J.E. was supported by a Royal Society Newton International Fellowship. The European Research Council (ERC Advanced Grant No. 695511, ENABLE), Fonds der Chemischen Industrie (Material Cost Allowance), Focus Area Nanoscale of the Freie Universität Berlin, Berlin University Alliance as part of the Oxford-Berlin Research Partnership (joint seed grant), and the Ministry of Culture and Science of the German state of North Rhine-Westphalia (NRW return program) are gratefully acknowledged for financial support. Open Access funding enabled and organized by Projekt DEAL.

Conflict of Interest

C.V.R. provides consultancy services for OMass Therapeutics. The authors declare no conflict of interest.

Data Availability Statement

The data that support the findings of this study are available in the supplementary material of this article.

Keywords: detergent · HLB · lipid · membrane · protein

[1] M. Rask-Andersen, M. S. Almén, H. B. Schiöth, *Nat. Rev. Drug Discovery* **2011**, *10*, 579–590.
[2] a) A. Laganowsky, E. Reading, T. M. Allison, M. B. Ulmschneider, M. T. Degiacomi, A. J. Baldwin, C. V. Robinson, *Nature* **2014**, *510*, 172–175; b) K. Gupta, J. A. C. Donlan, J. T. S. Hopper, P. Uzdavinys, M. Landreh, W. B. Struwe, D. Drew, A. J. Baldwin, P. J. Stansfeld, C. V. Robinson, *Nature* **2017**, *541*, 421–424; c) J. R. Bolla, J. B. Sauer, D. Wu, S. Mehmood, T. M. Allison, C. V. Robinson, *Nat. Chem.* **2018**, *10*, 363–371.
[3] a) R. Bilginer, A. Arslan Yildiz, *Biomimetic Lipid Membranes: Fundamentals, Applications, and Commercialization*. Kök F., Arslan Yildiz A., Inci F. (eds), Springer, Cham. **2019**, 1–306; b) L. H. Urner, *Curr. Opin. Chem. Biol.* **2022**, *69*, 102157.
[4] L. H. Urner, I. Liko, H.-Y. Yen, K. K. Hoi, J. R. Bolla, J. Gault, F. G. Almeida, M.-P. Schweder, D. Shutin, S. Ehrmann, R. Haag, C. V. Robinson, K. Pagel, *Nat. Commun.* **2020**, *11*, 564.
[5] a) S. J. Opella, F. M. Marassi, *Arch. Biochem. Biophys.* **2017**, *628*, 92–101; b) A. J. Miles, B. A. Wallace, *Chem. Soc. Rev.* **2016**, *45*, 4859–4872.
[6] M. Aivaliotis, P. Samolis, E. Neofotistou, H. Remigy, A. K. Rizos, G. Tsiotis, *BBA-Biomembranes* **2003**, *1615*, 69–76.
[7] A. A. Kermani, *FEBS J.* **2020**, *288*, 5788–5804.
[8] L. H. Urner, M. Schulze, Y. B. Maier, W. Hoffmann, S. Warnke, I. Liko, K. Folmert, C. Manz, C. V. Robinson, R. Haag, K. Pagel, *Chem. Sci.* **2020**, *11*, 3538–3546.
[9] B. Danielczak, S. Keller, *Methods* **2020**, *180*, 27–34.
[10] A. Laganowsky, E. Reading, J. T. S. Hopper, C. V. Robinson, *Nat. Protoc.* **2013**, *8*, 639–651.
[11] E. Reading, I. Liko, T. M. Allison, J. L. P. Benesch, A. Laganowsky, C. V. Robinson, *Angew. Chem. Int. Ed.* **2015**, *54*, 4577–4581; *Angew. Chem.* **2015**, *127*, 4660–4664.
[12] a) M. le Maire, P. Champeil, J. V. Möller, *Biochim. Biophys. Acta* **2000**, *1508*, 86–111; b) A. M. Seddon, P. Curnow, P. J. Booth, *Biochim. Biophys. Acta* **2004**, *1666*, 105–117; c) G. G. Privé, *Methods* **2007**, *41*, 388–397.
[13] a) A. J. Borysik, C. V. Robinson, *Phys. Chem. Chem. Phys.* **2012**, *14*, 14439–14449; b) A. J. Borysik, D. J. Hewitt, C. V. Robinson, *J. Am. Chem. Soc.* **2013**, *135*, 6078–6083.
[14] a) C. Bechara, C. V. Robinson, *J. Am. Chem. Soc.* **2015**, *137*, 5240–5247; b) K. Gupta, J. Li, I. Liko, J. Gault, C. Bechara, D. Wu, J. T. Hopper, K. Giles, J. L. P. Benesch, C. V. Robinson, *Nat. Protoc.* **2018**, *13*, 1106–1120; c) J. R. Bolla, R. A. Corey, S. Sahin, J. Gault, A. Hummer, J. T. S. Hopper, D. P. Lane, D. Drew, T. M. Allison, P. J. Stansfeld, C. V. Robinson, L. Landreh, *Angew. Chem. Int. Ed.* **2020**, *132*, 3551–3556.

[15] H. Ilgü, J.-M. Jeckelmann, M. S. Gachet, R. Boggavarapu, Z. Ucurum, J. Gertsch, D. Fotiadis, *Biophys. J.* **2014**, *106*, 1660–1670.
[16] C. Bechara, A. Nöll, N. Morgner, M. T. Degiacomi, R. Tampé, C. V. Robinson, *Nat. Chem.* **2015**, *7*, 255–262.
[17] L. H. Urner, A. Ariamajd, A. Weikum, *Chem. Sci.* **2022**, *13*, 10299–10307.
[18] W. C. Griffin, *J. Soc. Cosmet. Chem.* **1949**, *1*, 311–326.
[19] a) T. Vilgis, *Rep. Prog. Phys.* **2015**, *78*, 124602; b) S. Alam, M. S. Algahtani, M. Zaki Ahmad, J. Ahmad, *Cosmetics* **2020**, *7*, 1–12.
[20] J. E. Zajic, W. Seffens, *Biotechnology for the Oils and Fats Industry*, ed. C. Ratledge, P. Dawson, J. Rattray, American Oil Chemists' Society, USA, 1984, ch. **1921**, pp. 1241–1256.
[21] a) J. N. Umbreit, J. L. Strominger, *PNAS* **1973**, *70*, 2997–3001; b) L. H. Urner, I. Liko, K. Pagel, R. Haag, C. V. Robinson, *BBA-Biomembranes* **2022**, *1864*, 183958.
[22] a) L. H. Urner, Y. B. Maier, R. Haag, K. Pagel, *J. Am. Soc. Mass Spectrom.* **2019**, *30*, 174–180; b) L. H. Urner, K. Goltsche, M. Selent, I. Liko, M.-P. Schweder, C. V. Robinson, K. Pagel, R. Haag, *Chem. Eur. J.* **2021**, *27*, 2537–2542.
[23] L. H. Urner, E. Mohammadifar, K. Ludwig, D. Shutin, F. Fiorentino, I. Liko, F. G. Almeida, D. Kutifa, R. Haag, C. V. Robinson, *ACS Appl. Polym. Mater.* **2021**, *3*, 5903–5911.
[24] a) N. T. Johansen, F. G. Tidemann, M. C. Pedersen, L. Arleh, *Biochimie* **2022**, *205*, 3–26; b) H. J. Lee, H. S. Lee, T. Youn, B. Byrne, P. S. Chae, *Chem* **2022**, *8*, 980–1013.
[25] K. B. Steinbruch, M. Fridman, *MedChemComm* **2016**, *7*, 86–102.
[26] L. H. Urner, *Mus-Veteau, I. (eds) Heterologous Expression of Membrane Proteins. Methods in Molecular Biology, vol 2507*, Humana, New York, NY **2022**, 359–374.
[27] J. Gault, J. A. C. Donlan, I. Liko, J. T. Hopper, G. Kallol, N. G. Housden, W. B. Struwe, M. T. Marty, T. Mize, C. Bechara, Y. Zhu, B. Wu, C. Kleanthous, M. Belov, E. Damoc, A. A. Makarov, C. V. Robinson, *Nat. Methods* **2016**, *13*, 333–336.
[28] E. Nji, Y. Chatzikyriakidou, M. Landreh, D. Drew, *Nat. Commun.* **2018**, *9*, 4253.
[29] B. Trappmann, K. Ludwig, M. R. Radowski, A. Shukla, A. Mohr, H. Rehage, C. Böttcher, R. Haag, *J. Am. Chem. Soc.* **2010**, *132*, 11119–11124.
[30] E. Frotscher, B. Danielczak, C. Vargas, A. Meister, G. Durand, S. Keller, *Angew. Chem. Int. Ed.* **2015**, *54*, 5069–5073; *Angew. Chem.* **2015**, *127*, 5158–5162.
[31] a) K. H. Cho, H. E. Bae, M. Das, S. H. Gellman, P. S. Chae, *Chem. Asian J.* **2014**, *9*, 632–638; b) A. Marconnet, B. Michon, B. Prost, A. Solgadi, C. Le Bon, F. Giusti, C. Tribet, M. Zoonens, *Anal. Chem.* **2022**, *94*, 14151–14158; c) H. Hussain, T. Helton, Y. Du, J. S. Mortensen, P. Hariharan, M. Ehsan, B. Byrne, C. J. Loland, B. K. Kobilka, L. Guan, P. S. Chae, *Analyst* **2018**, *143*, 5702–5710.
[32] a) Q. Zhang, W.-X. Hong **2008**, PCT/US2008/012358; b) W.-X. Hong, K. A. Baker, X. Ma, R. C. Stevens, M. Yeager, Q. Zhang, *Langmuir* **2010**, *26*, 8690–8696; c) K. H. Cho, P. Hariharan, J. S. Mortensen, Y. Du, A. K. Nielsen, B. Byrne, B. K. Kobilka, C. J. Loland, L. Guan, P. S. Chae, *ChemBioChem* **2016**, *17*, 2334–2339; d) S. Lee, S. Ghosh, S. Jana, N. Robertson, C. G. Tate, N. Vaidehi, *Biochemistry* **2020**, *59*, 2125–2134; e) L. Liu, Z. Zhu, F. Zhou, D. Xue, T. Hu, W. Luo, Y. Qiu, D. Wu, F. Zhao, Z. Le, H. Tao, *ACS Omega* **2021**, *6*, 21087–21093; f) S. Hanashima, T. Nakane, E. Mizohata, *Membranes* **2021**, *11*, 823.
[33] P. S. Chae, A. C. Kruse, K. Gotfryd, R. R. Rana, K. H. Cho, S. G. F. Rasmussen, H. E. Bae, R. Chandra, U. Gether, L. Guan, B. K. Kobilka, C. J. Loland, B. Byrne, S. H. Gellman, *Chem. Eur. J.* **2013**, *19*, 15645–15651.
[34] D. R. Storm, S. O. Field, J. Ryan, *J. Supramol. Struct.* **1976**, *4*, 221–231.
[35] J. Breibeck, A. Rompel, *BBA - General Subject* **2019**, *1863*, 437–455.
[36] T. Youn, S. Yoon, B. Byrne, P. S. Chae, *ChemBioChem* **2022**, *23*, e2022002.
[37] E. Slinde, T. Flatmark, *BBA-Biomembranes* **1976**, *455*, 796–805.
[38] J. Gault, I. Liko, M. Landreh, D. Shutin, J. R. Bolla, D. Jefferies, M. Agasid, H.-Y. Yen, M. J. G. W. Ladds, D. P. Lane, S. Khalid, C. Mullen, P. N. Remes, R. Huguet, G. McAlister, M. Goodwin, R. Viner, J. E. P. Syka, C. V. Robinson, *Nat. Methods* **2020**, *17*, 505–508.
[39] H.-Y. Yen, K. K. Hoi, I. Liko, G. Hedger, M. R. Horrel, W. Song, D. Wu, P. Heine, T. Warne, Y. Lee, B. Carpenter, A. Plückthun, C. G. Tate, M. S. P. Sansom, C. V. Robinson, *Nature* **2018**, *559*, 423–427.
[40] F. Fiorentino, J. B. Sauer, X. Qiu, R. A. Corey, C. K. Cassidy, B. Mynors-Wallis, S. Mehmood, J. R. Bolla, P. J. Stansfeld, C. V. Robinson, *Nat. Chem. Biol.* **2021**, *17*, 187–195.
[41] A. von Kügelgen, H. Tang, G. G. Hardy, D. Kureisaite-Ciziene, Y. V. Brun, P. J. Stansfeld, C. V. Robinson, T. A. M. Bharat, *Cell* **2020**, *180*, 348–358.
[42] J. W. Patrick, C. D. Boone, W. Liu, G. M. Conover, Y. Liu, X. Cong, A. Laganowsky, *PNAS* **2018**, *115*, 2976–2981.
[43] H. S. Garmory, R. W. Titball, *Infect. Immun.* **2004**, *72*, 6757–6763.
[44] F. Fiorentino, J. R. Bolla, S. Mehmood, C. V. Robinson, *Structure* **2019**, *27*, 651–659.
[45] A. O. Oluwole, R. A. Corey, C. M. Brown, V. M. Hernández-Rocamora, P. J. Stansfeld, W. Vollmer, J. R. Bolla, C. V. Robinson, *Nat. Commun.* **2022**, *13*, 2278.
[46] D. S. Chorev, C. V. Robinson, *Nat. Chem. Biol.* **2020**, *16*, 1285–1292.
[47] N. Kobayashi, K. Nishino, A. Yamaguchi, *J. Bacteriol.* **2001**, *183*, 5639–5644.
[48] N. P. Barrera, S. C. Isaacson, M. Zhou, V. N. Bavro, A. Welch, T. A. Schaedler, M. A. Seeger, R. N. Miguel, V. M. Korkhov, H. W. van Veen, H. Venter, A. R. Walmsley, C. G. Tate, C. V. Robinson, *Nat. Methods* **2009**, *6*, 585–587.
[49] N. P. Greene, E. Kaplan, A. Crow, V. Koronakis, *Front. Microbiol.* **2018**, *9*, 50.
[50] S. Mehmood, J. Marcoux, J. T. S. Hopper, T. M. Allison, I. Liko, A. J. Borysik, C. V. Robinson, *J. Am. Chem. Soc.* **2014**, *136*, 17010–17012.
[51] M. Wyszogrodzka, R. Haag, *Chem. Eur. J.* **2008**, *14*, 9202–9214.

Manuscript received: January 17, 2023
Accepted manuscript online: March 10, 2023
Version of record online: April 19, 2023